QSAR, MOLECULAR DOCKING AND MD SIMULATION OF ISOXAZOLE-PIPERAZINE DERIVATIVES AS ANTICANCER AGENTS

Deepak Sharma[1] , Suchitra Yadav[2], Anuradha Sharma[3], Naincy Kaushal[4], Reshmi Kumari[5] , Mukul Arora[6] , and Balasubramanian Narasimhan[7]*

ABSTRACT

Hepatocellular carcinoma is the most common cause of death, having 75% of all primary liver malignancies worldwide. Luminespib (heat shock protein inhibitor) was found efficiently active against various tumours and hence acted as a key to the research. In this research isoxazole-piperazine derivatives were subjected to QSAR, molecular docking, and MD simulations studies. The QSAR results indicated the importance of First order molecular connectivity index (1χ; r= 0.775, q2 = 0.532) for MCF-7 cell line; Second-order molecular connectivity index (2χ; r = 0.880, q2 = 0.730) for Huh -7 cell line; Lowest unoccupied molecular orbital and Randic topological index (LUMO, R; r = 0.703 and q2 = 0.347) for Mahlavu cell line in describing the anticancer activity of isoxazole-piperazine derivatives. The significance of constructed models has been supported by statistical parameters. Further, molecular docking was done to understand the molecular interactions with the target protein human topoisomerase II (PDB ID: 3QX3), which predicted the anticancer activity against MCF-7, Huh-7 and Mahlavu cell lines. The docking results demonstrated that compounds 15, 7m, and 7f showed best docking score along with binding with crucial amino acid residues. Further, MD simulation was done for compounds 13c and 13d depending on their biological activities, docking score and molecular interactions with the target. The results of MD simulations showed stability of the compounds. Finally, these compounds may be used as a new lead for further discovery.

Keywords: QSAR, Molecular docking, MD simulations, Isoxazole-piperazine derivatives, Anticancer

[1,6]Faculty of Pharmaceutical Sciences, B.S. Anangpuria Institute of Pharmacy, Faridabad, Haryana, India – 121004

[2,3]Faculty of Pharmaceutical Sciences, Deen Dayal Rustagi College of Pharmacy, Gurgaon, Haryana, India – 122504

[4]Research Scholar of Microbial Technology, CSIR Institute of Microbial Technology, Chandigarh , India – 160036

[5]Resarch Scholar of Molecular Virology, King Institute of Preventive Medicine & Research, Tamil Nadu, India – 600032

[7*]Faculty of Pharmaceutical Sciences, Maharshi Dayanand University, Rohtak, Haryana, India – 124001

***Corresponding Author**

Prof. Balasubramanian Narasimhan

*Faculty of Pharmaceutical Sciences, Maharshi Dayanand University, Rohtak, Haryana, India – 124001

Email: naru2000us@yahoo.com

DOI: - 10.48047/ecb/2023.12.si5a.0512

INTRODUCTION

Cancer is a disease that dependence on multiple factors and is total result of hereditary, genetic, and environmental elements. It is the major causes of mortality worldwide. HCC is the common type of cancer, having 75% of all primary liver malignancies worldwide [1, 2]. Anticancer drug resistance is a complex process that arises from apoptosis suppression, altering in the drug targets and drug metabolism, gene amplification, epigenetic and genetic factors [3]. Drug resistance may be the reason why we have to put a never ending effort to identify and produce new and more potent anticancer drugs capable of intervening with these complicated processes.

Isoxazole based moieties are most essential for anticancer activity. Therapeutic activities of isoxazole moiety are anticancer [4], antifungal [5], herbicidal [6], anti-HIV [7], antitubercular [8], and insecticidal [9]. In isoxazole ring, O and N atom are present with adjacent connection, having low bond dissociation energy: N-N = 945.4 kj mol^{-1}, N-O = 630.7 kj mol^{-1}, and C-O = 1076.4 kj mol^{-1} [10]. Many compounds with a piperazine nucleus have been described as chemotherapeutic agents for types of cancer like colon cancer, prostate cancer, breast cancer, lung cancer, and leukemic carcinoma, etc [11].

In recent years, QSAR has earned significance in the field of medicinal chemistry, being an authentic predictive tool for evaluation of the activity of chemical compounds using CADD [12]. It is a method, in which mathematical equations produce a connection between structures and their biological activities [13].

Structure-based drug design approach include molecular docking and molecular dynamics simulation. Both these techniques show ligand-protein interactions by following different algorithms. The best docked pose has minimum free binding energy which indicates the ligand's binding propensity to form a stable complex with protein. MD simulations is a step forward from molecular docking, in which ligands find their places in the active site of a protein after a given number of confirmational moves in the binding pocket of the protein [14].

A series of isoxazole-piperazine compounds with an inhibitory effect against MCF-7 (breast cancer), Huh-7, Mahlavu cell line (liver cancer) was considered to carry out the research, which was suggested by the individual efficacy of isoxazole and piperazine derivatives as anticancer agents. The mechanism of action of compounds having isoxazole-piperazine hybrid ring is to arrest G1 or G2/ M phase of cell cycle and resulting in apoptotic cell death [11].

The above findings inspired us to perform QSAR, molecular docking and MD simulation studies to analyse the deeper insights of the isoxazole-piperazine derivatives.

MATERIALS & METHODS

Data Set

The data set of isoxazole-piperazine derivatives (6a-6t, 7a-7n, 13a-13d, 14, and 15) were drawn in Chem Draw Ultra software 12.0 and their energy was minimized. Anticancer activities given in IC_{50} in µM were converted to pIC_{50} (logarithmic units) as shown in Table 1, reported by Ibis *et. al.,* (2022) [11].

Table 1 Chemical Structure and their pIC50 values of Isoxazole-piperazine derivatives

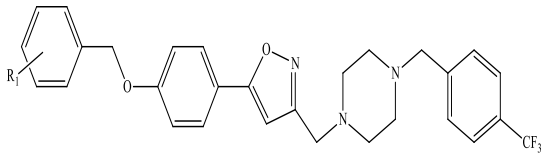

(6a-6t)

Compounds	R1	MCF-7	Huh-7	Mahlavu
6a	H	0.46	0.23	1.07
6b	2-Me	0.57	0.08	0.83
6c	3-Me	0.60	0.70	0.40
6d	4-Me	0.08	0.18	0.88
6e	3,5-diMe	0.20	-0.22	0.78
6f	2-Cl	0.45	0.00	0.51
6g	3-Cl	0.15	-0.70	0.61
6h	4-Cl	0.83	0.60	0.57
6i	2-CN	0.60	0.70	0.54
6j	3-CN	-0.10	-1.00	1.03
6k	4-CN	-1.00	0.00	0.63
6l	2-F	0.48	0.18	0.49
6m	3-F	0.40	0.11	0.46
6n	4-F	0.90	0.30	0.49
6o	2-OMe	-0.52	-0.05	0.59
6p	3-OMe	0.30	-0.10	0.15
6r	4-OMe	0.11	0.51	0.69
6s	3,5-diOMe	-1.00	0.18	0.63
6t	3,4,5-triOMe	0.26	-0.30	0.76

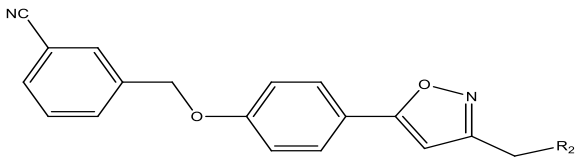

(7a-7n)

Compounds	R2	MCF-7	Huh-7	Mahlavu
7a	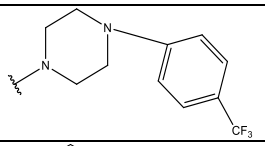	0.30	0.34	0.43
7b	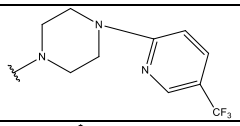	0.15	0.23	0.11
7c	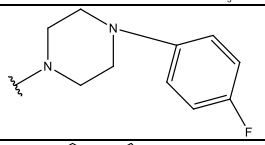	0.38	0.18	0.34
7d	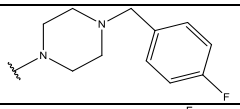	0.26	0.20	0.18
7e	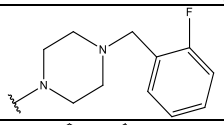	0.15	0.38	0.36
7f	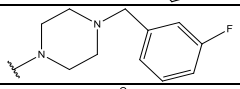	0.38	0.43	0.41
7g	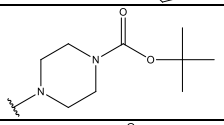	0.58	0.79	0.75
7h	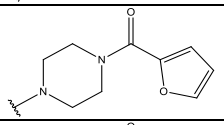	0.28	0.30	0.34
7i	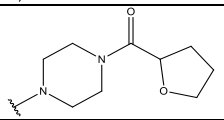	0.58	0.34	0.61
7j	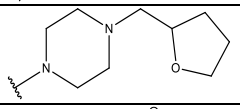	0.92	0.62	0.68
7k	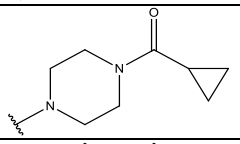	0.88	0.45	0.64
7l	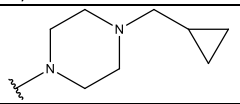	0.54	0.46	0.51
7m	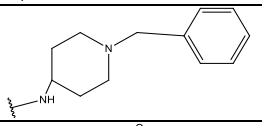	0.40	0.40	0.32
7n	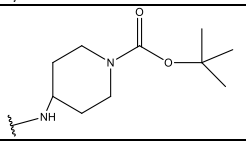	0.45	0.18	0.48

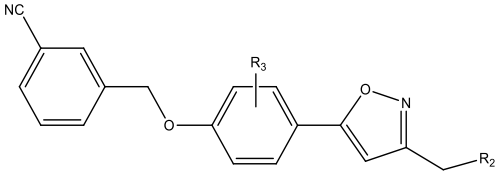

(13a-13d, 14, 15)

Compounds	R3	R2	MCF-7	Huh-7	Mahlavu
13a	2-Me	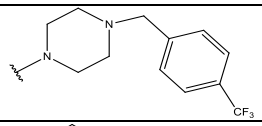	-0.40	0.18	-0.30
13b	3-Me	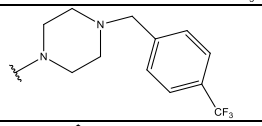	-0.15	-0.22	-0.35
13c	2-F	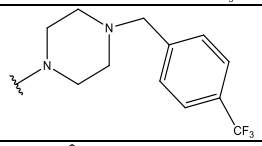	0.08	-0.40	-0.40
13d	3-F	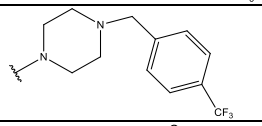	-0.42	-1.05	-0.30
14	3-F	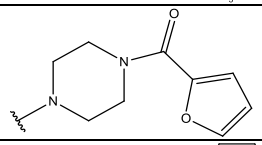	0.18	0.91	0.56
15	3-F	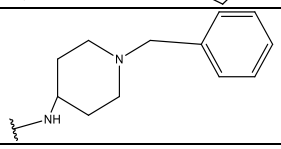	0.43	0.36	0.43

Generation of Descriptors and Regression Analysis

Further molecular descriptors were generated using the software TSAR 3.3 (Oxford Molecular 2000). Molecular descriptors which were considered in this research, were log of octanol-water partition coefficient (log P), Valence molecular connectivity indices ($^{0}\chi^{V}$, $^{1}\chi^{V}$, $^{2}\chi^{V}$, $^{3}\chi^{V}$) and Kier's shape indices ($k\alpha^{1}$, $k\alpha^{2}$, $k\alpha^{3}$), Randic topological index (R), Total energy (TE), Highest occupied molecular orbital (HOMO) and Lowest unoccupied molecular orbital (LUMO), Dipole moment (μ) for isoxazole-piperazine derivatives [12]. Pearson's correlation matrix was used to select the suitable descriptors for regression analysis. The forward selection method was further applied for the generation of regression model. Various outliers were removed as suggested by the work of Furusjö [15]

Table 2 Selected molecular descriptors used in QSAR studies

Comp.	**μ**	**log P**	**$^{1}\chi$**	**$^{1}\chi^{v}$**	**$^{2}\chi$**	**$^{2}\chi^{v}$**	**κ^{1}**	**$\kappa\alpha^{1}$**	**R**	**LUMO**
6a	6.366	6.271	17.920	12.259	16.743	9.228	28.526	25.737	17.920	-0.572
6b	6.413	6.738	18.331	12.676	17.261	9.669	29.491	26.697	18.331	-0.581
6c	6.422	6.738	18.314	12.670	17.377	9.732	29.491	26.697	18.314	-0.562
6d	6.279	6.738	18.314	12.670	17.365	9.728	29.491	26.697	18.314	-0.562
6e	6.375	7.205	18.708	13.080	18.023	10.239	30.458	27.659	18.708	-0.560
6f	5.590	6.789	18.331	12.773	17.261	9.774	29.491	26.976	18.331	-0.605
6g	6.384	6.789	18.314	12.767	17.377	9.844	29.491	26.976	18.314	-0.630
6h	6.051	6.789	18.314	12.767	17.365	9.841	29.491	26.976	18.314	-0.632
6i	4.651	6.136	18.869	12.649	17.452	9.511	30.458	27.168	18.869	-0.645
6j	7.015	6.136	18.852	12.643	17.546	9.555	30.458	27.168	18.852	-0.687
6k	6.645	6.136	18.852	12.643	17.534	9.551	30.458	27.168	18.852	-0.703
6I	5.480	6.410	18.331	12.365	17.261	9.334	29.491	26.630	18.331	-0.596
6m	6.386	6.410	18.314	12.359	17.377	9.372	29.491	26.630	18.314	-0.627
6n	6.028	6.410	18.314	12.359	17.365	9.369	29.491	26.630	18.314	-0.634
6o	3.922	6.018	18.869	12.788	17.452	9.554	30.458	27.620	18.869	-0.514
6p	3.251	6.018	18.852	12.782	17.546	9.594	30.458	27.620	18.852	-0.503
6r	6.368	6.018	18.852	12.782	17.534	9.591	30.458	27.620	18.852	-0.560
6s	6.863	5.765	19.784	13.305	18.361	9.963	32.395	29.510	19.784	-0.529

6t	5.059	5.513	20.749	13.840	18.985	10.276	34.338	31.406	20.749	-0.632
7a	2.549	6.041	18.369	12.197	17.099	9.116	29.491	26.207	18.369	-0.755
7b	3.666	5.892	18.369	12.057	17.099	8.974	29.491	26.524	18.369	-0.749
7c	4.505	5.297	17.157	11.569	15.141	8.547	26.601	23.471	17.157	-0.700
7d	3.666	5.892	18.369	12.057	17.099	8.974	29.491	26.524	18.369	-0.749
7e	6.475	5.392	17.657	12.021	15.484	8.951	27.563	24.426	17.657	-0.612
7f	5.989	5.392	17.641	12.015	15.600	8.990	27.563	24.426	17.641	-0.644
7g	4.612	4.239	16.786	11.671	15.863	9.551	28.019	25.307	16.786	-0.674
7h	8.103	3.641	17.174	11.408	15.024	8.353	26.601	23.433	17.174	-0.651
7i	3.942	3.023	17.174	11.984	15.024	8.911	26.601	23.929	17.174	-0.686
7j	7.036	3.708	16.747	11.992	14.613	9.020	25.641	23.290	16.747	-0.581
7k	4.275	3.466	16.174	11.368	14.317	8.683	24.684	22.063	16.174	-0.709
7l	5.927	4.186	15.747	11.376	13.906	8.828	23.728	21.427	15.747	-0.616
7m	5.574	5.066	17.747	12.426	15.308	9.225	27.563	24.493	17.747	-0.645
7n	5.782	4.052	17.286	12.181	16.204	9.930	28.994	26.278	17.286	-0.792
13a	4.155	6.603	19.263	13.060	18.076	10.011	31.426	28.131	19.263	-0.630
13b	8.365	6.603	19.263	13.060	18.086	10.007	31.426	28.131	19.263	-0.752
13c	4.312	6.275	19.263	12.749	18.076	9.676	31.426	28.063	19.263	-0.879
13d	3.789	6.275	19.263	12.749	18.086	9.672	31.426	28.063	19.263	-0.869
14	4.665	3.780	17.585	11.514	15.564	8.471	27.563	24.320	17.585	-0.837
15	3.642	5.206	18.157	12.531	15.848	9.342	28.526	25.383	18.157	-0.848

Molecular Docking

The whole data set was prepared using ligprep module of Schrodinger *v* 13.1, with the assistance of epik. The energy minimization of molecules was performed using force field $OPLS_5$ [16, 17].

Then, the protein target i.e., Human topoisomerase II β in complex with DNA and etoposide as inhibitor (PDB ID : 3QX3) was shortlisted [18]. Protein target was obtained from the protein data bank (PDB) (http://www.rcsb.org). Protein preparation wizard was used in the Schrodinger *v* 13.1. In which preprocess, optimization H-bond, and clean up of water molecules were performed using force field $OPLS_5$ [19].

Then, generation of grid was accomplished using receptor grid generation suit of Schrodinger *v* 13.1. All the default functions were used to get required output. In this step, a grid was generated around the interacting site of already tenanted ligand molecule to facilitate derivative of isoxazole-piperazine to bind at the same site in the target protein [20].

Finally, molecular docking was attempted to analyse the interactions of isoxazole-piperazine derivatives against Human topoisomerase II β using extra precision (XP) mode. Docking scores were analysed from the project table in the Schrodinger *v* 13.1 [21]. Interactions of docked compounds with target were analysed. Molecular docking outcomes were validated by comparing the docking score range (-5 to -15 kcal/ mol) and by computing RMSD of docked conformation of the bounded ligand with reference to the co-crystallized ligand tenanted in the crystal structure.

Molecular Dynamics Simulation

Any grid based docking approach has the drawback of treating the receptor as a rigid entity, resulting in a static image of the protein-ligand interaction. In the physiological system, however, this relationship is dynamics [22]. MD simulations were performed for 10 ns using the system builder panel in Desmond suit of Schrodinger *v* 13.1 using $OPLS_4$ force field. SPC water box was applied on the system along with orthorhombic boundaries [23]. The system was neutralized by adding Na+ as counter ions. Further, molecular dynamics panel of Desmond was used to run simulation calculations by adjusting simulation time, ensemble class, relax model system before simulation etc. All the default functions were used to run the calculations. The simulation results were analysed by RMSD and RMSF, protein-ligand interaction and contacts [23].

RESULTS AND DISCUSSION

QSAR Model

This research was designed to construct significant regression models to anticipate the correlation between the molecular descriptors mentioned in Table 2 of isoxazole-piperazine derivatives with their anticancer activity against three cell lines, these are MCF-7, Huh-7 and Mahlavu cell line on breast cancer and liver cancer Table 1 by MLR analysis.

QSAR Studies of Isoxazole-piperazine Derivatives against MCF-7

For MCF-7 cell lines, compounds 6k, 6s, 6h, 6n, 6o, 6t, 6i, 13d, 13a, 6c, 6b, and 7l were eliminated

as outliers because their presence led in low correlation (r = 0.567, Equation 1, Table 1) with first order molecular connectivity ($^1\chi$), whereas their elimination improved the r value drastically (r = 0.775, Equation 2) during linear regression analysis.

pIC_{50} (MCF-7) = - 0.259 $^1\chi$ + 4.969 (Eq. 1)
n= 39, r = 0.567, q^2 = 0.219, SD = 0.371, F = 0.0001

Outliers removed 6k, 6s, 6h, 6n, 6o, 6t, 6i, 13d, 13a, 6c, 6b, and 7l
pIC_{50} (MCF-7) = -0.244$^1\chi$ + 4.71 (Eq. 2)
n= 27, r = 0.775, q^2 = 0.532, SD = 0.160, F = 37.789
Here, n - the number of data points, r - the correlation coefficient, SD - the standard error of the estimate, F – the Fischer ratio, q^2 - the cross-validated, r^2 - obtained by loo method.

Table 3 Correlation matrix of isoxazole-piperazine derivative against MCF-7 as anticancer agents

	MCF-7	**μ**	**log P**	$^1\chi$	$^1\chi^v$	$^2\chi$	$^2\chi^v$	κ^1	$\kappa\alpha^1$	**R**	**LUMO**
MCF-7	1.000										
μ	-0.055	1.000									
log P	-0.286	0.109	1.000								
$^1\chi$	-0.567	-0.030	0.680	1.000							
$^1\chi^v$	-0.439	0.106	0.693	0.901	1.000						
$^2\chi$	-0.489	0.009	0.803	0.936	0.875	1.000					
$^2\chi^v$	-0.316	0.158	0.641	0.700	0.893	0.797	1.000				
κ^1	-0.546	-0.033	0.677	0.974	0.893	0.967	0.784	1.000			
$\kappa\alpha^1$	-0.502	-0.010	0.685	0.956	0.916	0.971	0.829	0.991	1.000		
R	-0.567	-0.030	0.680	1.000	0.901	0.936	0.700	0.974	0.956	1.000	
LUMO	0.044	0.361	0.254	0.050	0.251	0.108	0.224	0.029	0.104	0.050	1.000

The regression models demonstrated an inverse correlation between magnitude of anticancer activity and first order molecular connectivity index ($^1\chi$) of isoxazole-piperazine derivatives. A representation of the observed pIC_{50} and the predicted pIC_{50} showed the activity values were close to each other hence the model was significant and the existance of systemic error was determined by the observed pIC_{50} and the residual pIC_{50} graph. The propagation of residuals on both the sides of zero specified that there was no systemic error in the construction of the regression model (Fig. 1(a), (b)).

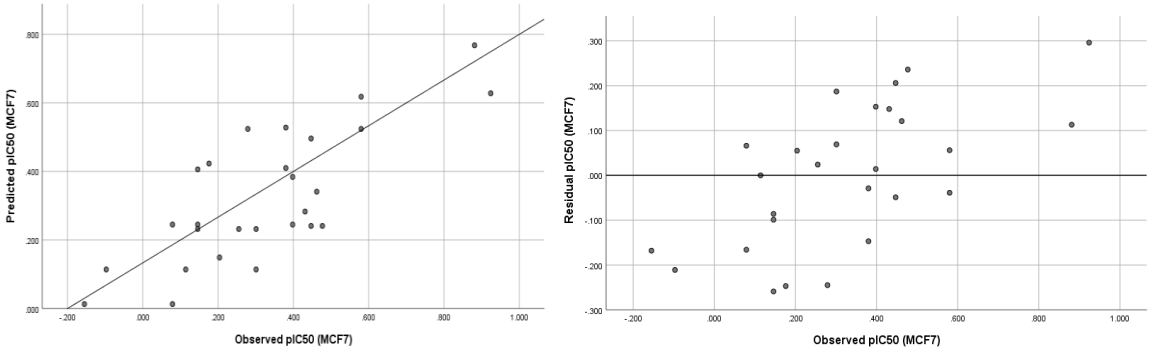

(a) **(b)**

Fig. 1 (a) Observed pIC_{50} (MCF-7) vs predicted pIC_{50} (MCF-7) and **(b)** Observed pIC_{50} (MCF-7) vs residual pIC_{50} MCF-7) MLR model (Equation 2).

QSAR Studies of Isoxazole-piperazine Derivatives against Huh-7

For Huh-7 cell lines, compounds 6j, 13d, 6g, 6i, 6c, 6h, 14, 6r, 7g, 13c, 6s, 7c, 13a, and 6h were eliminated as outliers because their presence led in low correlation (r = 0.522, Equation 3, Table 4) with second order molecular connectivity ($^2\chi$), whereas their elimination exceptionally improved the r value (r = 0.880, Equation 4) during linear regression analysis.

pIC_{50} (Huh7) = - 0.181 $^2\chi$ + 3.21 (Eq. 3)
n = 39, r = 0.522, q^2 = 0.205, SD = 0.373, F = 13.912

Outliers removed 6j, 13d, 6g, 6i, 6c, 6h, 14, 6r, 7g, 13c, 6s, 7c, 13a, and 6h
pIC_{50} (Huh7) = - 0.159 $^2\chi$ + 2.82 (Eq. 4)
n = 25, r = 0.880, q^2 = 0.730, SD = 0.115, F= 79.643

Table 4 Correlation matrix of isoxazole-piperazine derivatives against Huh-7 as anticancer agents

	Huh-7	**μ**	**log P**	$^{1}\chi$	$^{1}\chi^{v}$	$^{2}\chi$	$^{2}\chi^{v}$	κ^{1}	$\kappa\alpha^{1}$	**R**	**LUMO**
Huh-7	1.000										
μ	-0.047	1.000									
log P	-0.425	0.109	1.000								
$^{1}\chi$	-0.516	-0.030	0.680	1.000							
$^{1}\chi^{v}$	-0.489	0.106	0.693	0.901	1.000						
$^{2}\chi$	-0.522	0.009	0.803	0.936	0.875	1.000					
$^{2}\chi^{v}$	-0.437	0.158	0.641	0.700	0.893	0.797	1.000				
κ^{1}	-0.509	-0.033	0.677	0.974	0.893	0.967	0.784	1.000			
$\kappa\alpha^{1}$	-0.498	-0.010	0.685	0.956	0.916	0.971	0.829	0.991	1.000		
R	-0.516	-0.030	0.680	1.000	0.901	0.936	0.700	0.974	0.956	1.000	
LUMO	0.155	0.361	0.254	0.050	0.251	0.108	0.224	0.029	0.104	0.050	1.000

Equation 4 was found to best significant model among all others possibilities. The regression models demonstrated an inverse correlation between magnitude of anticancer activity and second order molecular connectivity index ($^{2}\chi$) of isoxazole-piperazine derivatives. The representation of the observed pIC_{50} and the predicted pIC_{50} showed that the activity values were close to each other and hence the model was significant and the existance of systemic error was obtained by the observed pIC_{50} and the residual pIC_{50} plot. The propagation of residuals on both the sides of zero specified that there is no systemic error in the construction of the regression model (Fig. 2 (a), (b)).

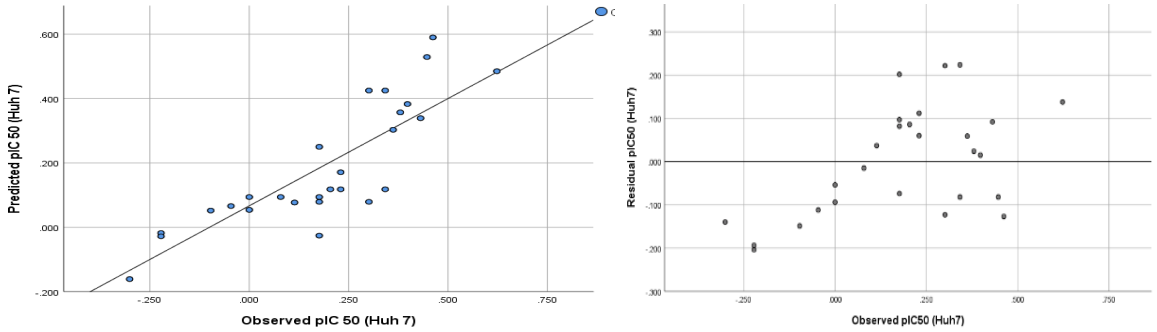

(a) **(b)**

Fig. 2 (a) Observed pIC_{50} (Huh-7) vs. predicted pIC_{50} (Huh-7) and **(b)** Observed pIC_{50} (Huh-7) vs. residual pIC_{50} (Huh-7) MLR model (Equation 4)

QSAR Studies of Isoxazole-piperazine Derivatives against Mahlavu

In Mahlavu cell line the linear regression analysis with entire dataset of 39 isoxazole-piperazine derivatives demonstrated the relevance of energy of the lowest unoccupied molecular orbital (LUMO) in reporting the anticancer activity (Equation 5, Table 5).

pIC_{50} (Mahlavu) = 1.700 LUMO + 1.580 (Eq. 5)

n = 39, r = 0.479, q^2 = 0.118, SD = 0.305, F =11.054

As the r value was very low which led to the lower inter-relationship between LUMO and other physicochemical parameters. This stimulated us to eliminate 13a, 6j, 13b, 6p, and 6t as outliers to get an equation with improved r value i.e., r = 0.479 to r = 0.657 as shown in Eq. 6.

pIC_{50} (Mahlavu) = 1.912 LUMO + 1.755 (Eq. 6)

n = 34, r = 0.657, q^2 = 0.303, SD = 0.219, F = 24.401

For the improvement of equation Randic topological index, as an independent variable was added, which led in drastic increase in r value from 0.657 to r= 0.703 as shown in Equation 7, Table 5.

pIC_{50} (Mahlavu) = - 0.081 LUMO + 1.932 R + 3.23 (Eq. 7)

n = 30, r = 0.703, q^2 = 0.347, SD = 0.210, F = 15.180

Table 5. Correlation matrix of isoxazole-piperzine derivatives against Mahlavu as anticancer agents.

	Mahlavu	**μ**	**Log P**	$^{1}\chi$	$^{1}\chi^{v}$	$^{2}\chi$	$^{2}\chi^{v}$	κ^{1}	$\kappa\alpha^{1}$	**R**	**LUMO**
Mahlavu	1.000										
μ	0.280	1.000									
Log P	-0.119	0.109	1.000								
$^{1}\chi$	-0.221	-0.030	0.680	1.000							
$^{1}\chi^{v}$	-0.076	0.106	0.693	0.901	1.000						
$^{2}\chi$	-0.167	0.009	0.803	0.936	0.875	1.000					
$^{2}\chi^{v}$	-0.026	0.158	0.641	0.700	0.893	0.797	1.000				
κ^{1}	-0.200	-0.033	0.677	0.974	0.893	0.967	0.784	1.000			
$\kappa\alpha^{1}$	-0.141	-0.010	0.685	0.956	0.916	0.971	0.829	0.991	1.000		
R	-0.221	-0.030	0.680	1.000	0.901	0.936	0.700	0.974	0.956	1.000	
LUMO	0.479	0.361	0.254	0.050	0.251	0.108	0.224	0.029	0.104	0.050	1.000

An inverse correlation was observed between anticancer activity and LUMO in regression model. In the above regression model, the value of q^2 was very low ($q^2 < 0.5$) which was validated by the fact that the only method to determine a model's actual predictive capability is by testing its ability to reliably anticipate the biological activities of compounds [24]. The graph of the observed pIC_{50} and the predicted pIC_{50} showed that the activity values are next to each other (Fig. 3 (a), (b)) and hence, the Equation 7 was significant. The exitance of systemic error was determined by the observed pIC_{50} and the residual pIC_{50} graph. The propagation of residuals on both the sides of zero specified that there was no systemic error in the construction of the regression model.

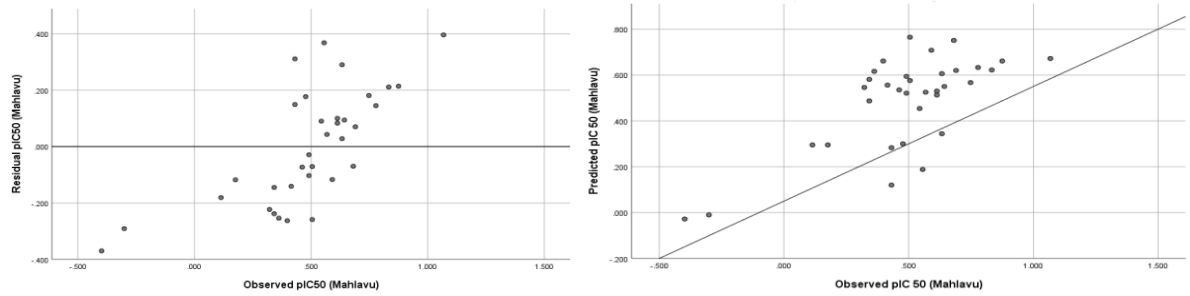

(a) **(b)**

Fig. 3 (a) Observed pIC_{50} (Mahlavu) vs. predicted pIC_{50} (Mahlavu) and **(b)** Observed pIC_{50} (Mahlavu) vs. residual pIC_{50} (Mahlavu) MLR model (Equation 7)

Molecular Docking

Target Identification

Human topoisomerase II β (DNA topoisomerase II) was identified as target for the given data set of isoxazole-piperazine [25]. Human topoisomerase II β (DNA topoisomerase II) cuts both ends of one DNA helix and then reanneals the cut strand. Topoisomerase II utilizing ATP energy. A dimer of Human topoisomerase II β in association with DNA and etoposide crystal structure. The protein and DNA dimer has 809 residues and is complexed with the anticancer drug etoposide. X-ray crystal or nuclear magnetic resonance should be used to determine the target structure, which can be acquired from the PDB website [26].

Table 6 Docking score and glide energy of isoxazole-piperazine derivatives and some control as anticancer agents

S. No.	**Compound**	**Docking Score**	**Glide Energy**	**S. No.**	**Compound**	**Docking Score**	**Glide Energy**
1	**15**	-8.892	-69.446	**22**	**6f**	-6.117	-60.341
2	**7m**	-8.354	-69.449	**23**	**7i**	-6.085	-68.67
3	**7f**	-8.146	-64.107	**24**	**13c**	-6.075	-69.226
4	**7k**	-7.822	-59.92	**25**	**13d**	-6.057	-66.57
5	**6b**	-7.75	-58.923	**26**	**7d**	-5.893	-57.183
6	**7h**	-7.555	-62.862	**27**	**6d**	-5.754	-59.399

7	**7g**	-7.515	-73.18	**28**	**6g**	-5.494	-62.567
8	**7e**	-7.455	-64.251	**29**	**6h**	-5.419	-58.851
9	**6e**	-7.398	-61.372	**30**	**6r**	-5.351	-57.637
10	**7c**	-7.349	-62.018	**31**	**6s**	-4.875	-65.359
11	**7l**	-7.161	-55.883	**32**	**13a**	-4.788	-67.215
12	**7j**	-7.112	-57.181	**33**	**6p**	-4.457	-62.96
13	**14**	-7.084	-68.974	**34**	**13b**	-4.197	-64.774
14	**6o**	-7.008	-62.989	**35**	**7b**	-3.872	-64.953
15	**6t**	-6.979	-71.344	**36**	**6a**	-3.385	-62.993
16	**6l**	-6.672	-61.529	**37**	**7n**	-3.377	-68.422
17	**6m**	-6.625	-55.57	**38**	**6i**	-2.585	-67.131
18	**6k**	-6.556	-67.76	**39**	**7a**	-1.955	-59.795
19	**6j**	-6.323	-59.949	**40**	**Luminespib (Control 1)**	-8.555	-62.541
20	**6n**	-6.319	-54.798	**41**	**Leflunomide (Control 2)**	-4.631	-39.816
21	**6c**	-6.137	-60.018				

Molecular Docking Results

Molecular docking studies were attempted to analyse the binding interactions of compounds against the target protein. Ligand interactions showed binding interactions of compounds and control (approved) drug in the active site of Human topoisomerase II β (chain A) (PDB ID: 3QX3) having a resolution of 2.16 Å was selected. Docking scores and glide energy for the whole data set is represented in Table 6, whereas their interactions with crucial amino acid binding residues in the binding pocket of the target is represented in Table 7. The docking score (binding affinity scoring function) of compounds 15, 7m, 7f, 13c, and 13d were considered with target protein and showed good to moderate anticancer activity. Binding interactions were found for compound 15, forming H-bonding with amino acid (Gln778) and had a good docking score (-8.892). Binding interactions were seen for compound 7m, forming H-bonding with a H_2O molecule and had a good docking score (-8.354). Binding interactions were observed for compound 7f, forming DT : D9 (pi-pi Stacking) and had a good docking score (-8.146). Binding interactions were found for compound 13c, forming H-Bonding with a water molecule, DT : D9, DG : F13 (pi-pi Stacking) and had a good docking score (-6.075). Binding interactions were seen for compound 13d, forming DT : D9 (pi-pi Stacking) and had a good docking score (-6.057). Then, with Luminespib (Control 1) there was DC : C8, DT : D9 (pi-pi stacking), DT : D9 (H-Bonding) observed with a good docking score (-8.555), whereas with Leflunomide Control 2 there was DT : D9 (pi-pi stacking), H_2O (H-bonding) observed with a good docking score (-4.631). From the docking score results it could be seen that the docking scores are within the range of (-5 to -15) kcal/mol, this leads us to validation of molecular docking methods. Also, another validating parameter i.e., overlay methods is checked by observing the RMSD values (0.37 Å), which have upper acceptable limit of 2 Å. Compound 15, 7m showed better docking score than control 1 whereas compounds 15, 7m and 7f showed better docking score than control 2. The docking score correlates their anticancer activity. In the 2D and 3D binding mode, type of interactions were depicted by different colours i.e., pi-pi cation (green), pi-cation (red), h-boding (pink), etc. are shown in Fig. [(4 to 10) (a) (b)] and the interaction matrix for all the amino acid residues and the compounds is provided in Figure 11.

In light of above analysis, we have considered MD simulation studies to further check the validity of the above findings. One must not forget that IC_{50} values provided by the author have a great significance in itself as all the work was done on laboratory scale. Therefore, those isoxazole-piperazine derivatives which had good anticancer activities in all three cell lines (MCF-7, Huh-7 and Mahlavu) were further considered for the MD simulation studies.

Table 7 Docking score and interactions of top docked and most biologically active compounds and control drugs

S. No.	Compounds	Docking score	Glide energy	Interactions	Important interactions
1	**15**	-8.892	-69.446	Met382, Vel785, Asn786, Gln789, Gly812, Gly813, Lys814, Ala816, Pro819, Gln778, Arg503, Gly504, GLy478, Asp479,	Gln778 (H-bonding)
2.	**7m**	-8.354	-69.449	Glh477, Gly478, Asp479, Gly504, Arg503, Gln778, Pro819, Ser818, Ala816, Lys814, Gly813, Gly812, Gln789, Asn786, Val 785, Met782, DG : C5, DG : C8, DA : F12, DG : F 13, DT : D 9, DG : D10	H_2O (H- Bonding)
3.	**7f**	-8.146	-64.107	Gln778, Pro819, Ser818, Ala816, Lys814, Gly813, Gln789, Asn786, Val785, Met782, Arg503, Gly504, Asp409, Gly478, Glh477, DT:D9, DG : D10, DC : F11, DA : F12, DG : F13	DT: D9 (pi- pi Stacking)
4.	**13c**	-6.075	-69.226	Arg503, DG : F13, DA : F12, DC : F11, DC : C8, Gln778, DG:C5, Met82, Val785, Asn786, Gln789, Gly : 813, Lys814, Ala816, Ser818, Pro819, DT:D9	H_2O (H- Bonding), DT : D9, DG : F13 (pi- pi Stacking)
5.	**13d**	-6.057	-66.57	Ala816, Lys814, Gyl813, Gly812, Gln789, Asn786, Val785, Met782, Gln778, DC : C8, Gly504, Arg503, DA : F12, DG : F12, Asp479, DG : D10, DT : D9	DT : D9 (pi- pi Stacking)
6.	**Luminespib Control 1**	-8.555	-62.541	Lys456, Gly504, Arg503, Leu502, Asp479, Gly478, Glh477, Ile565, Gln778, DC : C8, DC : D11, DG : D10, DT : D9, DA : F12, DG : F13	DC : C8 , DT : D9 (pi- pi stacking) Dt D 9 (H-Bonding)
7.	**Leflunomide Control 2**	-4.631	-39.816	Leu502, Arg503, Gly504, Gly478, Glh477, Gln778, DC : C8, DT : D9, DG : F13, DA : F12,	DT : D9 (pi- pi stacking), H_2O (H- Bonding)

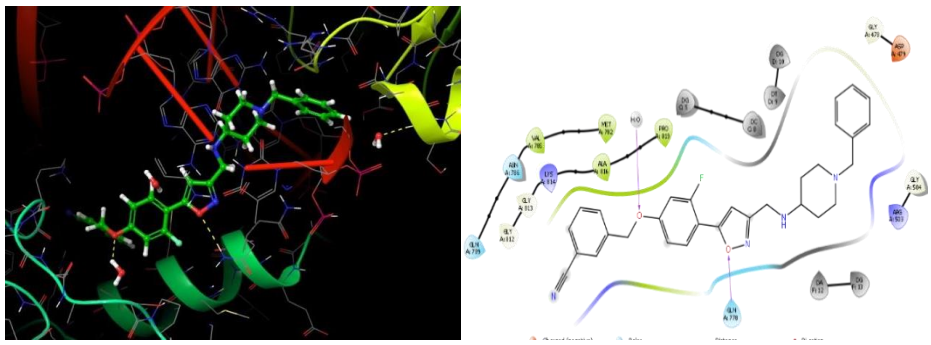

Figure 4 (a) 3D and (b) 2D binding interactions of Compound 15 within the active site of target (3QX3)

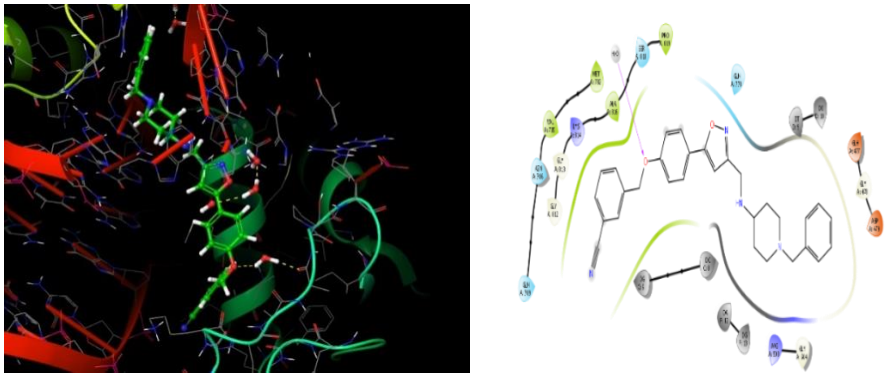

Figure 5 (a) 3D and (b) 2D binding interactions of Compound 7m within the active site of target (3QX3)

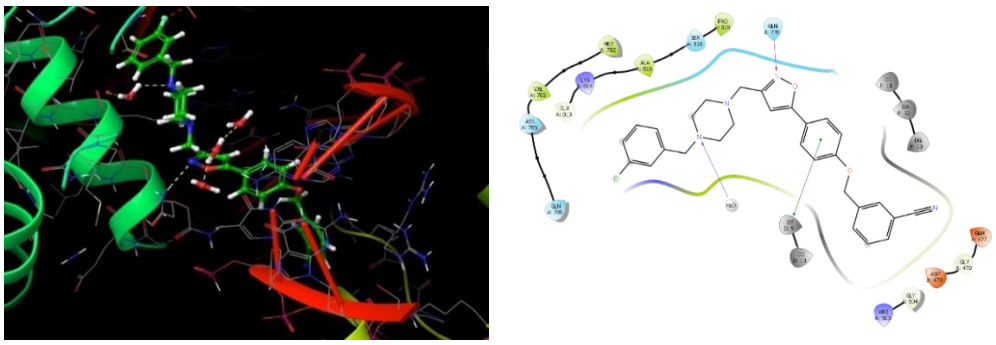

Figure 6 (a) 3D and (b) 2D binding interactions of Compound 7f within the active site of target (3QX3)

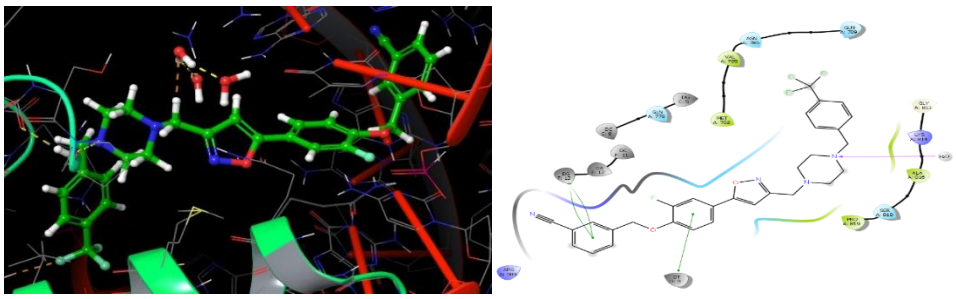

Figure 7 (a) 3D and (b) 2D binding interactions of Compound 13c within the active site of target (3QX3)

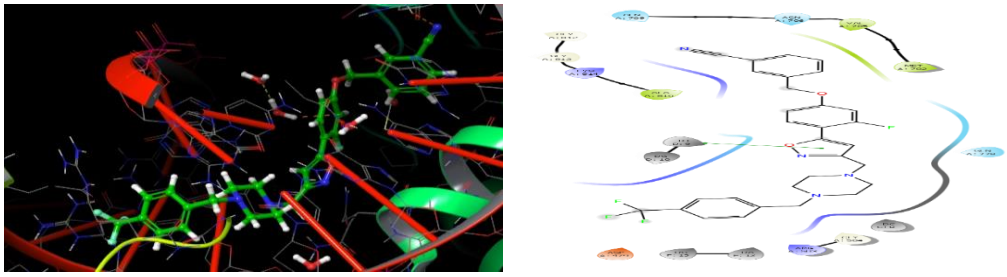

Figure 8 (a) 3D and (b) 2D binding interactions of Compound 13d within the active site of target (3QX3)

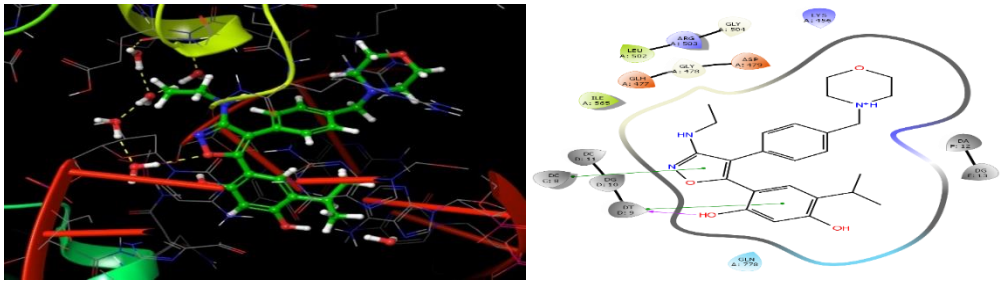

Figure 9 (a) 3D and (b) 2D binding interactions of Luminespib (Control 1) within the active site of target (3QX3)

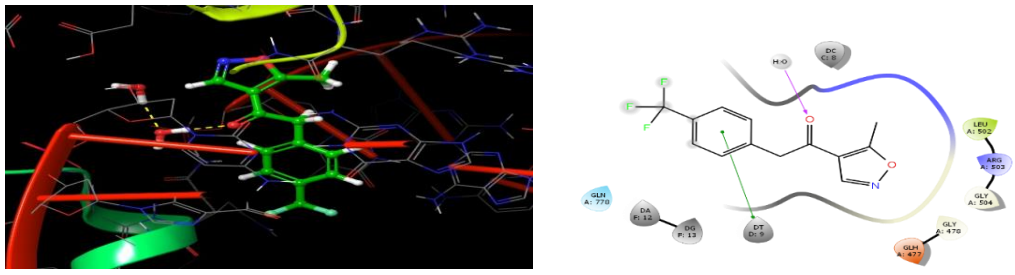

Figure 10 (a) 3D and (b) 2D binding interactions of Leflunomide (Control 2) within the active site of target (3QX3)

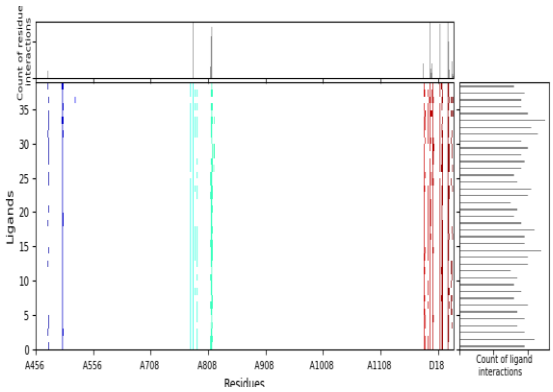

Figure 11 Interaction matrix of isoxazole-piperazine derivatives

Molecular Dynamics Simulations

Molecular dynamics (MD) simulation were performed for compounds 13c and 13d considering their biological activity i.e., IC_{50} values and analysed deeper binding insights with Human topoisomerase II β receptor (3QX3). The compound 13c showed protein RMSD values in the range (2.1-3.8) Å and ligand RMSD values in the range of (2.0-3.8) Å with fluctuations at various interval of time. The RMSD graph tells us stability of the protein-ligand complex, which is verified by lesser is the RMSD greater is the stability (Fig. 12 (a)). The RMSF values lies in the range (0.7-6.4) Å. The RMSF graph depicts the mobility of target proteins, with frequent peaks shows the presence of flexible amino acids on the c-alpha backbone of the protein. (Fig. 12 (b)). MD simulation outcomes specify probable protein-ligand interactions in form of histograms and heat maps (Fig. 12 (c), (d)). The interface between protein and ligand comprises four types of bonds, hydrogen bonds (green), hydrophobic interaction (grey), ionic bonds (pink), and water bridges (blue). The amino acid residues Gln778 forms H-bonds (green), Arg503, Met781, Met782, Val785, Lys814, Pro819 forms hydrophobic interaction (grey), and Glu477, Arg503, Gly776, Gln778, Met781 forms water bridges (blue) respectively (Fig. 12 (c)). Further individual interactions residue with the protein of trajectory frames is provided in the form of heat map. The intensity of colours indicates the interactions of amino acid. Amino acid Arg503, Met78 and Lys814 are having maximum no. of contact with given amino acid resides (Fig. 12 (e)). The residue Lys 814 showed 25% interaction whereas Arg503 showed 23% interaction more than 20% of time by forming H-bonding and water bridge with the ligand molecules respectively (Fig. 12 (d)).

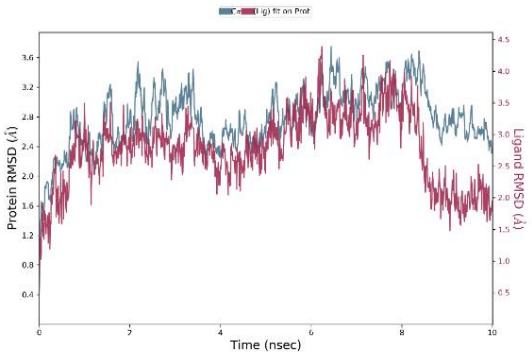

(a)

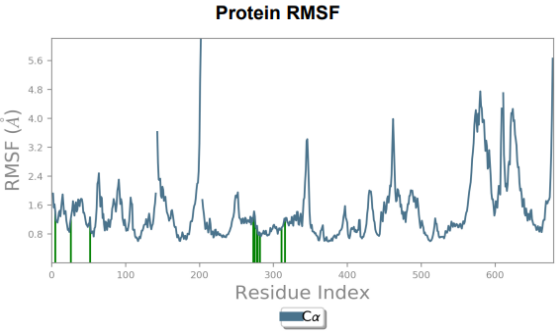

(b)

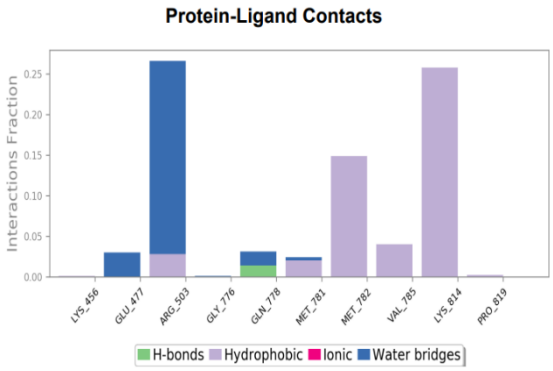

(c)

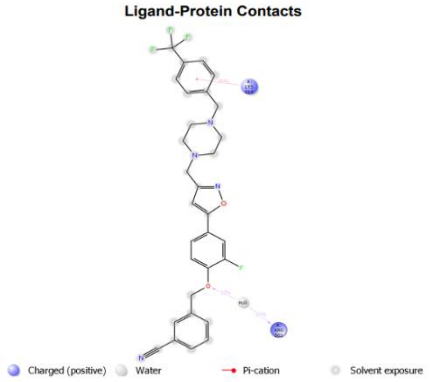

(d)

(e)

Figure 12 Compound 13c (a) Graphical representation of Protein RMSD (Å)and Ligand RMSD (Å) versus time (ns), (b) Graphical representation of RMSF (Å) versus residual index, (c) Histogram representation specify probable protein- ligand interactions, (d) Ligand protein contact, (e) Heat map showing protein-ligand interactions

The compound 13d showed protein RMSD values in the range (2.0-4) Å and ligand RMSD values in the range of (1.6-3.6) Å with fluctuations at various interval of time (Fig. 13 (a)). The RMSF values lies in the range (0.7-4.8) Å (Fig. 13 (b)). MD simulation outcomes specify probable protein-ligand interactions in form of histograms and heat maps (Fig. 13 (c), (d)). The amino acid residues Gln 778 forms H- bonds (green), Met781, Met782, Val785, Lys814 forms hydrophobic interaction (grey), and Gln778, Gln789, Phe806, Gly812, Gly813, Lys814, Ser818, Pro819 forms water bridges (blue) respectively (Fig. 13 (c)). Further individual interactions residue with the protein of trajectory frames is provided in the form of heat map. The intensity of colour indicates the interactions of amino acid. Amino acid Gln778, Met782, Val785, Gln789 are having maximum no. of contact with given amino acid resides (Fig.13(e)). The residue Gln779 showed 31% interaction and Gly813 showed 21% interaction more than 20% of time by forming water bridge with the ligand molecules (Fig. 13 (d)).

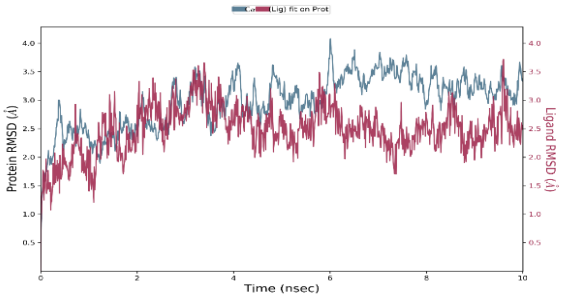

(a)

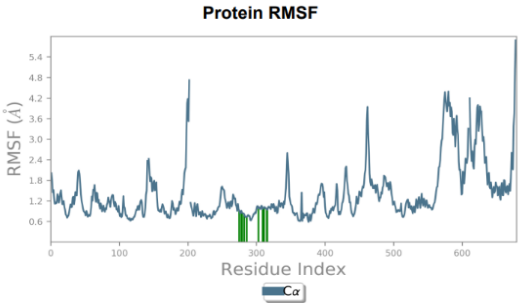

(b)

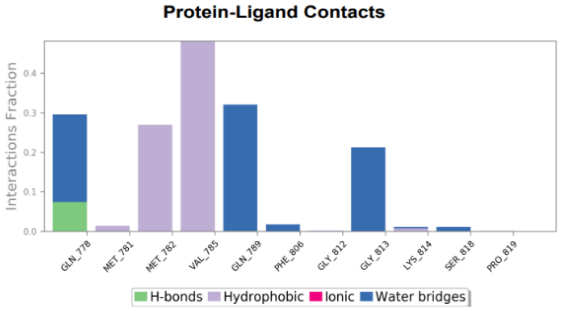

(a)

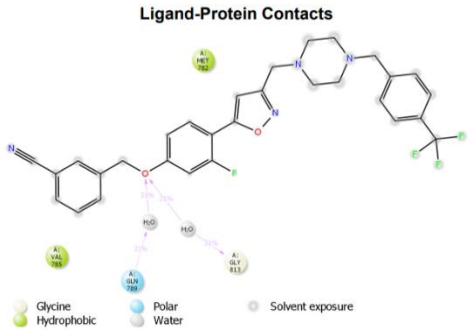

(b)

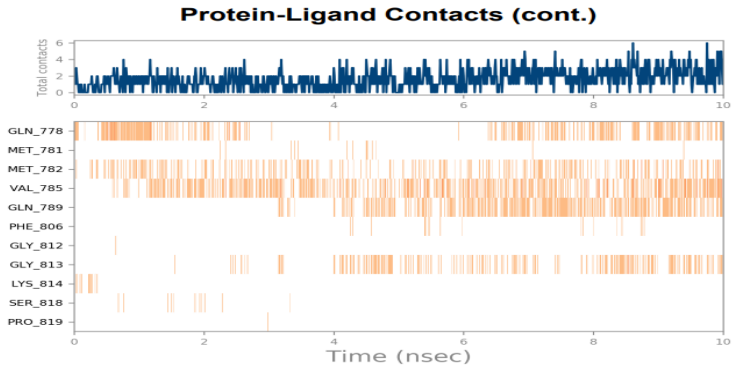

(e)

Figure 13 Compound 13d (a) Graphical representation of Protein RMSD (Å)and Ligand RMSD (Å) versus time (ns), (b) Graphical representation of RMSF (Å) versus residual index, (c) Histogram representation specify probable protein- ligand interactions, (d) Ligand protein contact, (e) Heat map showing protein-ligand interactions

CONCLUSION

The research was done to carry out QSAR studies, molecular docking and molecular simulation studies of isoxazole-piperazine derivatives using different computational approaches. QSAR results indicated the importance of first order molecular connectivity index ($^{1}\chi$) (r = 0.775, q^2 = 0.532) for MCF-7 cell line; second order molecular connectivity index ($^{2}\chi$) (r = 0.880, q^2 = 0.730) for Huh-7 cell line; lowest unoccupied molecular orbital and randic topological index (LUMO & R) (r = 0.703, q^2 = 0.347) for Mahlavu cell line in describing anticancer activity of isoxazole-piperazine derivatives. The inference of above QSAR models is that structural requirement for different anticancer target will be different. The molecular docking results showed compounds 15, 7m, and 7f showed significant docking scores, glide energy and showing interactions with various amino acids which ensuring better to moderate anticancer activity at specifies protein target (3QX3). Along with these compounds, some other compounds having moderate anticancer activity in the mentioned cell lines, docking score and binding interactions were considered for MD simulation (Compounds 13c and 13d). Simulations results showed significant and acceptable ranged outcomes hence show stability of the molecules. QSAR models, molecular docking and MD simulations results advise us that selected compounds of isoxazole-piperazine derivatives can be developed as more potent anticancer agents with various new modifications and can be major topic in successful treatment of chemotherapy for selected protein Human topoisomerase II β (PDB ID: 3QX3).

Abbreviations

IC_{50} : Half-maximal inhibitory concentration; pIC_{50} : Negative log of half-maximal inhibitory concentration; RMSD : Root Mean Square Deviation; RMSF : Root Mean Square Fluctuations; Obs : Observed; Pred : Predicted; MLR : Multiple Linear Regression; LOO : Leave One Out; PDB : Protein Data Bank; Ns : Nanosecond; MCF-7 : Michigan Cancer Foundation-7; Huh-7 : Hepatocyte derived cellular carcinoma; SPC : Simple Point Charge

Acknowledgements

The authors thank the Head of the Department of Pharmaceutical Sciences, Maharshi Dayanand University, Rohtak, for providing the necessary facilities to carry out this research work—special thanks to Mr. Vinod Devaraji and his team for guiding and learning Schrodinger software.

Authors' Contributions

Authors DS and BN designed the computational study; DS, BN and SY carried out the 2D QSAR study; AS and NK carried out the molecular docking study; RK and MA carried out the molecular dynamics simulation of synthesised compounds; BN helped in critical revision of the manuscript. All authors read and approved the final manuscript.

Funding

Not applicable

Availability of data and materials

The datasets used and analysed during the current study are available from the corresponding author upon reasonable request.

Ethics approval and consent to participate

Not applicable

Conflict of interest
The authors declare no conflict of interest

Consent for publication
All authors of the research paper have approved the manuscript for submission.

Author details
[1,6]Faculty of Pharmaceutical Sciences, B.S. Anangpuria Institute of Pharmacy, Faridabad, Haryana, India – 121004. [2,3]Faculty of Pharmaceutical Sciences, Deen Dayal Rustagi College of Pharmacy, Gurgaon, Haryana, India – 122504. [4]Research Scholar of Microbial Technology, CSIR Institute of Microbial Technology, Chandigarh , India – 160036. [5]Research Scholar of Molecular Virology, King Institute of Preventive Medicine & Research, Tamil Nadu, India – 600032. [7]Faculty of Pharmaceutical Sciences, Maharshi Dayanand University, Rohtak, Haryana, India – 124001.

REFERENCES

1. Sun, B.; Karin, M. Obesity, inflammation, and liver cancer. J. Hepatol. 2012 Mar 1;56(3):704-13.
2. Baffy, G.; Brunt, EM.; Caldwell, SH. Hepatocellular carcinoma in non-alcoholic fatty liver disease: an emerging menace. J. Hepatol. 2012 Jun;56(6):1384-91.
3. Mansoori, B.; Mohammadi, A.; Davudian, S.; Shirjang. S.; Baradaran, B. The different mechanisms of cancer drug resistance: a brief review. APB. 2017 Sep;7(3):339.
4. Misra, RN.; Xiao, HY.; Williams, DK.; Kim, KS.; Lu, S.; Keller, KA.; Mulheron, JG.; Batorsky, R.; Tokarski, JS.; Sack, JS.; Kimball, SD. Synthesis and biological activity of N-aryl-2-aminothiazoles: potent pan inhibitors of cyclin-dependent kinases. Bioorganic Med. Chem. Lett. 2004 Jun 7;14(11):2973-7.
5. Zhang, MZ.; Chen, Q.; Xie, CH.; Mulholland, N.; Turner, S.; Irwin, D.; Gu, YC.; Yang, GF.; Clough, J. Synthesis and antifungal activity of novel streptochlorin analogues. Eur. J. Med. Chem. 2015 Mar 6;92:776-83.
6. Li, G.; Qian, X.; Cui, J.; Huang, Q.; Zhang, R.; Guan, H. Synthesis and herbicidal activity of novel 3-aminocarbonyl-2-oxazolidinethione derivatives containing a substituted pyridine ring. J. Agric. Food Chem. 2006 Jan 11;54 (1): 125-9.
7. Ghosh, AK.; Takayama, J.; Kassekert, LA.; Ella-Menye, JR.; Yashchuk, S.; Agniswamy, J; Wang, YF.; Aoki, M.; Amano, M.; Weber, IT.; Mitsuya, H. Structure-based design, synthesis, X-ray studies, and biological evaluation of novel HIV-1 protease inhibitors containing isophthalamide-derived P2-ligands. Bioorganic Med. Chem. Lett. 2015 Nov 1;25(21):4903-9.
8. Li, D.; Gao, N.; Zhu, N.; Lin, Y.; Li, Y.; Chen, M.; You, X.; Lu, Y.; Wan, K.; Jiang, JD.; Jiang, W. Discovery of the disubstituted oxazole analogues as a novel class anti-tuberculotic agents against MDR-and XDR-MTB. Bioorganic Med. Chem. Lett. 2015 Nov 15;25 (22):5178-81.
9. Guo, P.; Huang, JH.; Huang, QC.; Qian, XH. Synthesis of novel 1, 3-oxazole derivatives with insect growth-inhibiting activities. Chin Chem Lett. 2013 Nov 1;24(11):957-61.
10. Arya, GC.; Kaur, K.; Jaitak, V. Isoxazole derivatives as anticancer agent: A review on synthetic strategies, mechanism of action and SAR studies. Eur. J. Med. Chem. 2021 Oct 5; 221:113511.
11. İbiş, K.; Nalbat, E.; Çalışkan, B.; Kahraman, DC.; Cetin-Atalay, R.; Banoglu, E. Synthesis and biological evaluation of novel isoxazole-piperazine hybrids as potential anti-cancer agents with inhibitory effect on liver cancer stem cells. Eur. J. Med. Chem. 2021 Oct 5;221:113489.
12. Kaushik, CP.; Kumar, K.; Narasimhan, B.; Singh, D.; Kumar, P.; Pahwa, A. Synthesis, antimicrobial activity, and QSAR studies of amide-ester linked 1, 4-disubstituted 1, 2, 3-triazoles Monatsh. Chem. 2017 Apr;148(4): 765-79.
13. Abbasi, M.; Sadeghi-Aliabadi, H.; Amanlou, M. 3D-QSAR, molecular docking, and molecular dynamic simulations for prediction of new Hsp90 inhibitors based on isoxazole scaffold. J. Biomol. Struct. Dyn. 2018 Apr 26; 36(6):1463-78.
14. Tripathi, A.; Misra, K. Molecular docking: A structure-based drug designing approach. JSM Chem. 2017;5(2):1042-7.
15. Furusjö, E.; Svenson, A.; Rahmberg, M.; Andersson, M. The importance of outlier detection and training set selection for reliable environmental QSAR predictions. Chemo sphere. 2006 Mar 1;63(1):99-108.
16. Madhavi, Sastry G.; Adzhigirey, M.; Day, T.; Annabhimoju, R.; Sherman, W. Protein and ligand preparation: parameters, protocols, and influence on virtual screening enrichments. J. Comput. Aided Mol. Des. 2013 Mar;27(3):221-34.
17. Van Den Driessche, G.; Fourches, D. Adverse drug reactions triggered by the common HLA-B* 57: 01 variant: a molecular docking study. J.

Cheminformatics. 2017 Dec;9(1):1-7.
18. Cherukumalli, PK.; Tadiboina, BR.; Gulipalli, KC.; Bodige, S.; Gangarapu, K.; Sridhar, G. Design, Synthesis, and Anticancer Activity of Bis-isoxazole Incorporated Benzothiazole Derivatives. Russ. J. Gen. Chem. 2020 Oct;90 (10):1981-9.
19. Kumar, S.; Singh, J.; Narasimhan, B.; Shah, SA.; Lim, SM.; Ramasamy, K.; Mani, V. Reverse pharmacophore mapping and molecular docking studies for discovery of GTPase HRas as promising drug target for bis-pyrimidine derivatives. Chem. Cent. J. 2018 Dec;12(1):1-1.
20. Sharma, V.; Sharma, PC.; Kumar, V. In silico molecular docking analysis of natural pyridoacridines as anticancer agents. Adv Chem. 2016 Nov;2016:1-9.
21. Friesner, RA.; Banks, JL.; Murphy, RB.; Halgren, TA.; Klicic, JJ.; Mainz, DT.; Repasky, MP.; Knoll, EH.; Shelley, M.; Perry, JK.; Shaw, DE. Glide: a new approach for rapid, accurate docking and scoring. 1. Method and assessment of docking accuracy. J. Med. Chem. 2004 Mar 25;47(7):1739-49.
22. Uniyal, A.; Mahapatra, MK.; Tiwari, V.; Sandhir, R.; Kumar, R. Targeting SARS-CoV-2 main protease: structure based virtual screening, in silico ADMET studies and molecular dynamics simulation for identification of potential inhibitors. J. Biomol. Struct. Dyn. 2022 May 24;40(8):3609-25.
23. Mukherjee, S.; Abdalla, M.; Yadav, M.; Madhavi, M.; Bhrdwaj, A.; Khandelwal, R.; Prajapati, L.; Panicker, A.; Chaudhary, A.; Albrakati, A.; Hussain, T. Structure-Based Virtual Screening, Molecular Docking, and Molecular Dynamics Simulation of VEGF inhibitors for the clinical treatment of Ovarian Cancer. J. Mol. Model. 2022 Apr;28(4):1-21.
24. Shen, M.; LeTiran, A.; Xiao, Y.; Golbraikh, A.; Kohn, H.; Tropsha, A. Quantitative structure− activity relationship analysis of functionalized amino acid anticonvulsant agents using k nearest neighbor and simulated annealing PLS methods. J. Med. Chem. 2002 Jun 20;45 (13):2811-23.
25. Yang, X.; Li, W.; Prescott, ED.; Burden, SJ.; Wang, JC. DNA topoisomerase IIβ and neural development. Science SAS. 2000 Jan 7;287(5450):131-4.
26. Sharma, KK.; Singh, B.; Mujwar, S.; Bisen, PS. Molecular docking based analysis to elucidate the DNA topoisomerase IIβ as the potential target for the ganoderic acid; a natural therapeutic agent in cancer therapy. Curr. Comput. Aided Drug Des. 2020 Apr 1;16 (2):176-89.